

# MAGNETIC CONFIGURATION EFFECTS ON TURBULENCE DRIVEN TRANSPORT FROM LHD AND W7X IDENTICAL EXPERIMENTS

K. TANAKA

National Institute for Fusion Science, National Institutes on Natural Sciences  
Toki, Japan  
Email: ktanaka@nifs.ac.jp

M. NUNAMI, M. NAKATA, T. TSUJIMURA, M. YOSHINUMA, H. IGAMI, Y. YOSHIMURA, H. TAKAHASHI, R. YANAI, T. SHIMOZUMA, M. YOKOYAMA, R. SEKI, S. SATAKE, H. SUGAMA, T. TOKUZAWA, R. YASUHARA, Y. TAKEMURA, H. FUNAMBA, I. YAMADA, K. IDA, B. PETERSON, Y. SUZUKI, S. KUBO, C. SUZUKI, M. OASKABE, T. MORISAKI

National Institute for Fusion Science, National Institutes on Natural Sciences  
Toki, Japan

F. WARMER, P. XANTHOPOULOS, G.G. PLUNK, M. N. A. BEURSKENS, G. M. WEIR, P. HELANDER, C.D. BEIDLER, T. STANGE, H. M. SMITH, D. ZHANG, Y. TURKIN, J. BRUNNER, A. STECHOW, J. GEIGER., A. LANGENBERG, E. PASCH, G. FUCHERT, S. BOZHENKOV, E. SCOTT, H. LAQUA, R.C. WOLF

Max-Planck-Institut für Plasmaphysik Greifswald  
Greifswald, Germany

Y. OHTANI

Naka Fusion Institute, National Institutes for Quantum and Radiological Science and Technology  
Naka, Japan

H. YAMADA

University of Tokyo  
Kashiwa, Japan

N. PABLANT

Princeton Plasma Physics Laboratory  
Princeton, New Jersey, USA

## Abstract

Characteristics of the turbulence driven transports are investigated in LHD and W7-X. The gyrokinetic non-linear simulation with identical input gradient shows lower ETG driven transport in W7-X and lower ITG driven transport in LHD. The configuration scan experiments in LHD shows that reduced transport associated with reduction of ion scale turbulence at inwardly shifted configuration, where effective helical ripple is low. The identical experiment between W7-X and LHD with similar density and heating power shows clear different density and temperature profiles. Total transport is lower in W7-X at most of the radial location, however, anomalous contribution is lower in LHD. The reduced ion transport in LHD qualitatively agree with gyrokinetic simulation. The effective helical ripple is not ruling parameter to reduce anomalous transport among stellarator/heliotron configuration.

## INTRODUCTION

Stellarator/heliotron is an alternative concept to tokamak for the future fusion reactor. Disruption free and no need to sustain plasma current to keep configuration are great advantages for stable steady state operation. In spite of these advantages, technical difficulty of manufacturing three-dimensional coil and generally degraded confinement characteristics compared with tokamaks H mode are issues to realize stellarator/heliotron reactors. Presently working two large stellarator/heliotron devices are Large Helical Device (LHD) in Toki, Japan starting in 1998 and Wenderstein 7-X (W7-X) in Greifswald, Germany starting in 2015. The two leading devices has proven the technical feasibility of three dimensional super conducting coils. However, characteristics of

confinements and its physics mechanism are not well understood enough for the design of next generation stellarator/heliotron devices. Historically, classical stellarators suffer from enhanced neoclassical transports due the magnetic helical ripple in particular in low collisionality regime [1]. The regime of enhanced neoclassical transport is called  $1/\nu$  regime, where  $\nu$  is electron-ion collisionality. In  $1/\nu$  regime, the neoclassical transport is proportional to  $\epsilon_{\text{eff}}$ , where  $\epsilon_{\text{eff}}$  is effective helical ripple, which is defined numerically converting multiple ripples to single ripple component. One of the design strategies of the stellarator/heliotron is to minimize neoclassical transport reducing  $\epsilon_{\text{eff}}$ . The configuration of LHD is close to the classical stellarators, however, inwardly positioning of plasma enables reduction of  $\epsilon_{\text{eff}}$ , then the neoclassical transport is almost one order magnitude lower compared with classical stellarator like configuration [2]. In W7-X, further optimization were performed then. Then, neoclassical diffusivity is one order magnitude lower in W7-X than in LHD at  $\rho > \sim 0.5$  for same collisionality [3].

There are plenty of theoretical investigations about anomalous transport in stellarator/heliotron. In LHD, one of the important messages is coincidence of the reduction of neoclassical transport and reduction of anomalous transport. Lower  $\epsilon_{\text{eff}}$  reduces neoclassical transport in  $1/\nu$  regime and simultaneously generates higher zonal flow [4]. The theoretical comparison between different magnetic configurations, where one is magnetic axis position ( $R_{\text{ax}}$ ) to be 3.6m, and the other to be 3.75m were performed.  $R_{\text{ax}}=3.6\text{m}$  is close to neoclassically optimized configuration and widely used for the experiments due to the good accessibility of the heating and moderate interaction with plasma inner wall.  $R_{\text{ax}}=3.75\text{m}$  is close to the classical stellarator configuration. The linear growth rate is higher at  $R_{\text{ax}}=3.6\text{m}$  than at  $R_{\text{ax}}=3.75\text{m}$  with identical input density and temperature gradient, however, nonlinear saturation level of ion temperature gradient (ITG) turbulence is lower at  $R_{\text{ax}}=3.6\text{m}$  than at  $R_{\text{ax}}=3.75\text{m}$  [5]. The results qualitatively account for the better global energy confinement at  $R_{\text{ax}}=3.6\text{m}$  than at  $R_{\text{ax}}=3.75\text{m}$  [6].

In W7-X, the maximum J, where J is the second adiabatic invariant, at plasma centre stabilizes the trapped electron mode (TEM) turbulence [7]. Recent gyrokinetic simulation account for the pellet enhanced performance, which is transient confinement improvement likely due to peaked density gradient [8]. Investigations from the comparisons between two devices will provide comprehensive understanding for the optimization of stellarator/heliotron. In Section 2, survey of gyrokinetic simulation of ITG turbulence and electron temperature gradient (ETG) turbulence are shown. In section 3, the configuration dependence are shown. The configuration dependence in W7-X are summarized from published material and configuration dependences in LHD are described from experiment. Then, the comparison of transport characteristics for the identical condition between LHD and W7-X are described in section 4. Finally, summary are shown in section 5.

## 1. GYROKINETIC INVESTIGATIONS IN LHD AND W7X

Figure 1 show three-dimensional plasma view of LHD at magnetic axis position ( $R_{\text{ax}}$ ) 3.6m and W7-X at standard configuration. In LHD, major radius (R) is 3.6m and minor radius (a) is 0.6m. Elliptical cross section rotates along toroidal direction keeping double null divertor configuration. Magnetic configurations are produce and can be tuned by the pair of helical winding coils and three pairs of vertical field coil. In W7-X, the major radius is 5.5m and the minor radius is 0.5m. The non-planar and planar coils are used to generate magnetic fields for the confinement. Around plasma boundary, natural magnetic islands are formed can be used for the multi-X point divertor placing target plate. The total volume is both  $30\text{ m}^3$ . Both devises use liquid helium cooled super conducting coils, which are designed for steady state operation.

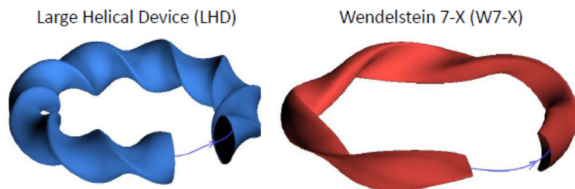


FIG. 1 Three dimensional view of plasma Large Helical Device (LHD) and Wenderstein 7-X ( W7-X)

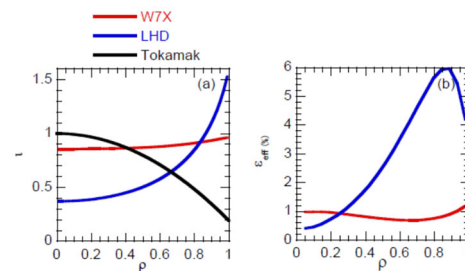


FIG. 2 Comparison of (a) rotational transform ( $\iota$ ) and (b) effective helical ripple ( $\epsilon_{\text{eff}}$ ).  $\iota$  profile in tokamak is shown as a reference.  $\epsilon_{\text{eff}}$  is zero in tokamak. LHD is (magnetic axis position)  $R_{\text{ax}}=3.6\text{m}$ , W7-X is standard configuration

Figure 2 shows comparison of the rotational transform ( $\iota$ ) and effective helical ripple ( $\epsilon_{\text{eff}}$ ). LHD is characterized by the high helical ripple and high magnetic shear, while W7-X is characterized by low helical ripple and low magnetic shear. The strong magnetic shear in LHD can reduce linear growth rate of ITG turbulence [9]. It should be noted that the sign of iota shear in both devices is opposite to a typical tokamak iota profile. Electron temperature gradient (ETG) turbulence contribute the electron transport when radial streamer is formed. However, the positive  $\iota$  shear can break radial streamer [10]. In tokamak,  $\epsilon_{\text{eff}}$  is very small. While in in heliotron/stellarator,  $\epsilon_{\text{eff}}$  is non zero and finite  $\epsilon_{\text{eff}}$  enhance neoclassical transport. Higher  $\epsilon_{\text{eff}}$  at outer region in LHD results in enhanced neoclassical transport in this region.

In order to investigate the configuration effects on turbulence driven transport, gyrokinetic non-linear analyses were performed for LHD and W7-X [11]. Experimental profiles of density and temperature under identical conditions are quite different as described in Sec. 4. The nonlinear saturation level is sensitive to input temperature gradient due to the temperature stiffness. Thus, same normalized temperature and density gradients were used in order to find the configuration effects clearly. For the simulation of LHD, GKV code [12] were used and for simulation of W7-X, GENE code were used [13]. In order to argue the ion and electron scale turbulence, ITG and ETG are simulated separately. For ITG simulation, adiabatic response of electrons were assumed and for ETG simulation, adiabatic response of ions were assumed. The normalized temperature gradient of ions ( $R/L_{Ti}$ ) and electrons ( $R/L_{Te}$ ) are assumed to be 3 for ITG and ETG simulation respectively. These simulations were performed separately for ITG and ETG, thus, the effects of interaction between ITG and ETG. The normalized density gradient ( $R/L_n$ ) were assumed to be 0.

Figure 3 shows non-linear ion heat flux driven by ITG and non-linear electron heat flux driven by ETG. As shown in Fig.3, the ITG driven ion heat flux is clearly lower in LHD than in W7-X. This is because zonal flow is more strongly generated in LHD and the ExB shearing rate due to zonal flow exceeds the linear growth rate of ITG in LHD. On the other hand, the ExB shearing rate due to zonal flow is much lower than linear growth rate of ITG in W7-X [11]. The results indicate that LHD configuration works better to reduce ITG turbulence. It should be noted that lower  $\epsilon_{\text{eff}}$  configuration in LHD generates larger zonal flow and results in reduced transport. If this strategy is applied for LHD and W7-X, W7-X should reduce ITG driven transport much more than LHD. However, results do not follow this story. Thus,  $\epsilon_{\text{eff}}$  is not only ruling parameter to reduce ITG driven transport, but there should be magnetic parameters.

In contrast to ITG driven ion heat flux, ETG driven electron heat flux is lower in W7-X than in LHD. Since the ETG is not affected by zonal flow [14], LHD configuration does not help to reduce ETG driven electron heat flux. In the previous study of ETG, radial streamers are broken for positive  $\iota$  shear devices such as positive  $\iota$  shear tokamak (negative  $q$  shear) and W7-X [10]. Such breaks of radial streamer was also found in this ETG simulation of LHD. It should be noted that  $\iota$  shear is higher in LHD but ETG driven electron transport is lower in W7-X. This result suggests that  $\iota$  shear is not only ruling parameter to determine ETG driven transport. In W7-X, ETG driven transport is more than one order magnitude lower than ITG driven transport and ETG does not contribute the transport in the case  $R/L_{Te}$  and  $R/L_{Ti}$  are identical [10]. This condition is realized in plasma edge region.

## 2. CONFIGURATION SCANS

In W7-X, configuration scan was carried out for standard, high-mirror and high-iota configurations [15]. The max-J properties are higher in high mirror and high-iota configuration than in standard configuration. The profile matching experiments showed lower anomalous thermal conductivities in higher mirror configuration than in standard and lower in high-iota than in standard configurations at  $\rho = 0.2 \sim 0.5$

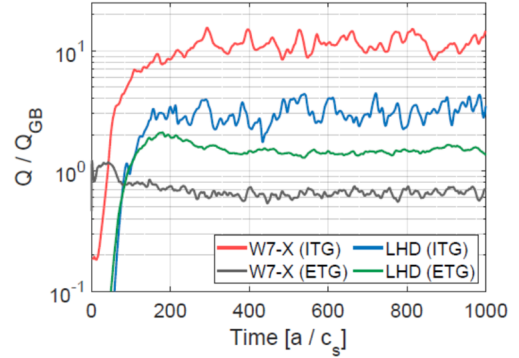


FIG. 3 Ion heat fluxes from ITG turbulence simulations ( $a/L_{Ti} = 3$ ;  $a/L_n = 0$ ) and electron heat fluxes from ETG turbulence simulations ( $a/L_{Te} = 3$ ;  $a/L_n = 0$ ) for W7-X and LHD. The fluxes are normalized to standard gyro Bohm units. Here,  $c_s$  denotes the ion sound speed and  $a$  is the minor radius. The time axis for the ETG simulations has been rescaled for visual purposes [11].

suggesting max-J works to stabilize TEM. However, the difference was unclear and within the estimation uncertainty at  $\rho = 0.5\sim 0.65$  [15].

In LHD, three configurations (Rax=3.6, 3.75 and 3.9m) are compared in low  $\beta$  ECRH plasma. Figure 4 shows  $\iota$ ,  $\epsilon_{\text{eff}}$  and normalized neoclassical transport coefficients. As shown in Fig.4 (a),  $\iota$  shear increases at more outwardly shifted configurations. In LHD, the averaged magnetic curvature is bad curvature in the edge region. Such magnetic hill region is narrower in more outwardly shifted configuration. However, in the present comparison experiments, such MHD stability characteristics does not affect the transport due to low  $\beta$ . As shown in Fig. 4. (b),  $\epsilon_{\text{eff}}$  increases significantly at more outwardly shifted configuration. The higher  $\epsilon_{\text{eff}}$  results in enhanced neoclassical transport as shown in Fig.4 (c).

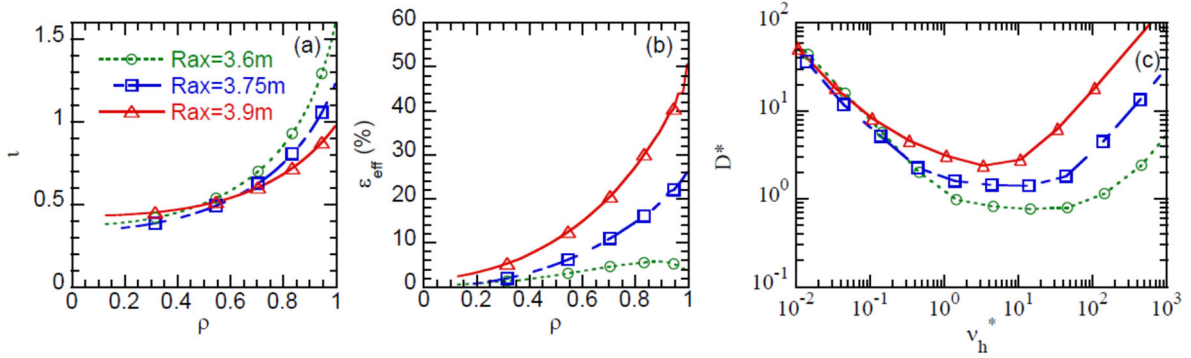


FIG. 4 Comparison of (a) rotational transform ( $\iota$ ) and (b) effective helical ripple ( $\epsilon_{\text{eff}}$ ) and (c) neoclassical diffusivities. In  $D^*=D_{\text{neo}}/D_p$ , The  $D_{\text{neo}}$  is monoenergetic neoclassical transport coefficients.  $D_p$  is the plateau value of the equivalent tokamak [2].  $v_h^* = v_{ei}/(\epsilon_{\text{eff}}^{3/2} v_T/qR_{mj})$ .  $v_{ei}$  is the electron ion collision frequency,  $v_T$  is the electron thermal velocity,  $q$  is the safety factor,  $R_{mj}$  is the major radius, and  $\epsilon_{\text{eff}}$  is an effective helical ripple.  $v_h^*=1$  corresponds to boundary between  $1/v$  and plateau regime.

For the identical experiments, the magnetic field at magnetic axis was adjusted to be 2.5T. This is technically possible maximum identical magnetic field strength for three configurations. Two megawatt 154GHz 2<sup>nd</sup> harmonic and 1.5 MW 77GHz fundamental heating was applied. The deposition location was  $\rho = 0.4$  at Rax=3.6 and 3.75m and  $\rho = 0.5$  at Rax=3.9m. ECRH was injected tangentially. The perpendicular injection from horizontal port was not possible due to the lack of the resonance. Two 154GHz gyrotrons and two 77 GHz gyrotrons were injected in balance in order to minimize ECCD current. Although the injection power was identical, the absorption power slightly varied due to the difference of shine through radiation. They are 3.4MW at Rax=3.6m, 3.2MW at Rax=3.75m and 2.9MW at Rax=3.9m.

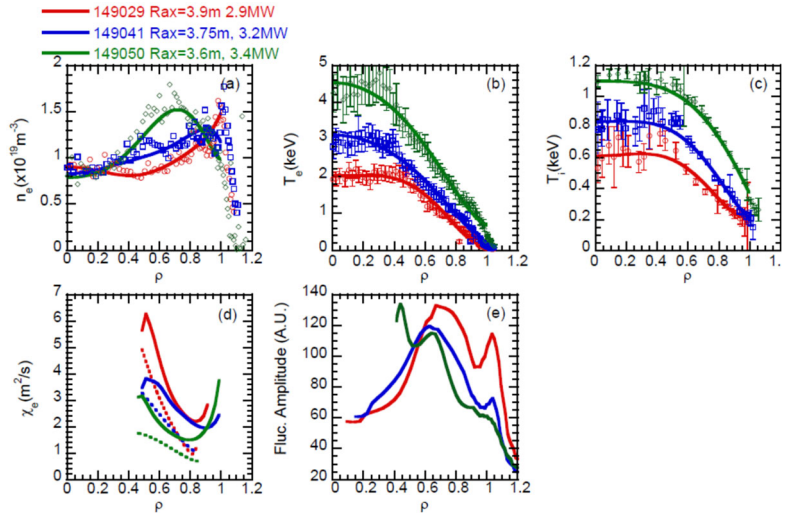


FIG. 5 Comparisons of profiles in identical experiments. (a)  $n_e$ , (b)  $T_e$ , (c)  $T_i$ , (d)  $\chi_e$  and (e) fluctuation amplitude. In (a), typical error bar is about 10~15% of the measured value. (a), (b), (c), (d) are time averaged for 4.1-5.0sec. In (d), experimental  $\chi_e$  were shown by plain line and neoclassical  $\chi_e$  were shown by dashed line

Figure 5 shows comparisons of profiles. The electron density ( $n_e$ ) and temperature ( $T_e$ ) were measured by Thomson scattering [16] and ion temperature ( $T_i$ ) was measured by charge exchange spectroscopy [17]. As shown in Fig. 5 (a),  $n_e$  profiles are all hollowed and hollowed region is more wider in outwardly shifted configuration. The hollowed density profile in LHD can be explained by neoclassical thermo-diffusion [18, 19]. The hollower profile at more outwardly shifted configuration can be due to the larger neoclassical thermo-diffusion at outwardly shifted configuration. As shown in Fig.5 (b) and (c),  $T_e$  and  $T_i$  are clearly higher at inwardly shifted configurations. The clearly higher  $T_e$  and  $T_i$  are not due to the difference of deposition power but due to the difference of transport.

The experimental electron thermal conductivities ( $\chi_e$ ) were evaluated by TASK3D code[20]. The ion deposition power was less than 10% of electron deposition power, thus, ion thermal conductivities ( $\chi_i$ ) cannot be evaluated accurately then they are not shown. The neoclassical values were evaluated by GSRAKE [3]. As shown in Fig.5 (d), both experimental and neoclassical  $\chi_e$  is lower at more inwardly shifted configuration. Ion scale turbulence  $k_{\text{perp}}\rho_i=0.1\sim 1$ , where  $k_{\text{perp}}$  is wavenumber perpendicular to magnetic field,  $\rho_i$  is ion Larmor radius, were measured by the two-dimensional phase contrast imaging (2D-PCI) [21,22]. As shown in Fig.5 (e), fluctuation amplitude is the lowest at  $R_{\text{ax}}=3.6\text{m}$ , then,  $R_{\text{ax}}=3.75\text{m}$  and the highest at  $R_{\text{ax}}=3.9\text{m}$ . The lower experimental  $\chi_e$  corresponds to lower fluctuation amplitude. These results support theoretical investigations [5], which shows simultaneous reduction of neoclassical transport and turbulence driven transport.

### 3. IDENTITY EXPERIMENTS IN LHD AND W7-X

In order to investigate the role of magnetic configuration in LHD and W7-X experimentally, identical experiments were carried out. The line averaged density ( $n_{e,\text{bar}}$ ) was  $\sim 3 \times 10^{19} \text{m}^{-3}$ . In LHD, ECRH was 154GHz 2<sup>nd</sup> harmonic heating, while in W7X, 140GHz 2<sup>nd</sup> harmonic heating. In both devices, ECRH was central heating and more than 90% injection power deposited within  $\rho = 0.2$ . The configurations of LHD was inwardly shifted configuration, where magnetic axis position was 3.6m at 2.75T. W7X was standard configuration at 2.5T. In the data sets, the volume averaged  $\langle \beta \rangle$  was less than 0.5% and plasma was free from macroscopic MHD activities.

Figure 6 shows comparisons of profiles. As shown in Fig.6 (a), density profiles are clearly different. It is hollowed in LHD and peaked in W7-X. The difference of the density profiles can be the difference of neoclassical thermo-diffusion, which is much higher in LHD. Figure 6 (b) and (c) shows  $T_e$  and  $T_i$  profiles. The normalized gradients of  $T_e$  and  $T_i$  is higher in W7X than in LHD, but, both  $T_e$  and  $T_i$  are higher in LHD at edge region, where  $n_e$  is higher in LHD. In LHD, turbulence was measured by 2D-PCI [22] and also linear analyses were carried out at  $\rho = 0.5$  and  $0.7$  [26]. Ion scale turbulence ( $k_{\text{perp}}\rho_i \sim 0.35$ ) exists at  $\rho > 0.4$  [26]. Also, microwave high k backscattering, which measures ETG region turbulence [27], showed clear signal at  $\rho = 0.7$  [26]. At  $\rho = 0.5$  and  $0.7$  both ITG and ETG were unstable [26]. In W7-X, linear analyses were not performed yet, but closed values of  $a/L_n$ ,  $a/L_{T_e}$  and  $a/L_{T_i}$  at  $\rho \sim 0.7$  as shown in Fig. 4 (d) suggests that linearly stable region so-called stability valley [28] may exists at this location.

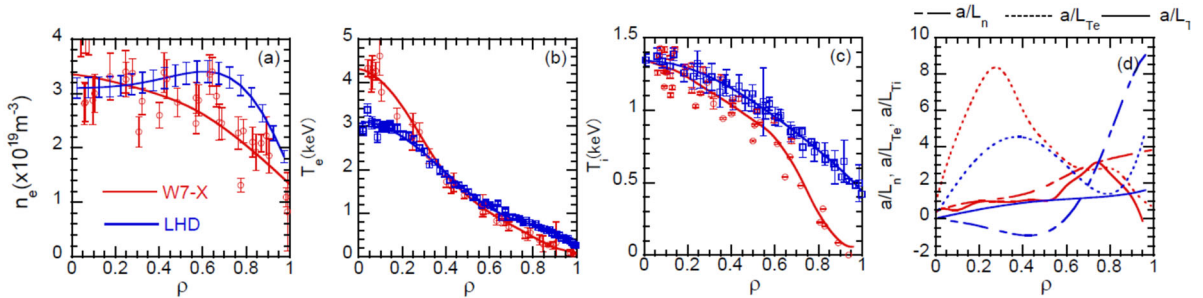


FIG.6 Comparisons of profiles (a) electron density ( $n_e$ ), (b) electron temperature ( $T_e$ ) (c) ion temperature ( $T_i$ ) and (d) normalized gradient of  $n_e$ ,  $T_e$  and  $T_i$ . In LHD,  $n_e$  was measured by far infrared interferometer[23], in W7-X by Thomson scattering [24].  $T_e$  and  $T_i$  were measured by Thomson scattering [16,24] and charge exchange spectroscopy [17,25].

LHD 152270 time averaged 4.3-4.8sec, W7-X 20180919.005

Figure 7 shows comparisons of integrated power from power balance analyses. Deposition power to electron and ion are shown. Also, neoclassical contribution is shown as well. In W7-X, the results of analyses are shown at  $\rho < 0.7$ , where the  $T_i$  gradients are well defined. In LHD, the results of analyses are shown at  $\rho < 0.8$ , where  $T_e > T_i$ .

Higher  $T_i$  than  $T_e$  is not physically acceptable since ion heating is only equipartition heating. The ion deposition power is due to the equipartition heating. The ion deposition power is higher than electron deposition power at  $\rho \sim 0.5$  in both devices. The contribution of neoclassical transport is quite different. In W7-X, neoclassical contribution is negligibly small at  $\rho > 0.5$ . On the other hand, the neoclassical contribution is quite large in LHD. In electron channel, 20~50% of electron power is dominated by neoclassical transport. In ion channel, deposition power is close to neoclassical contribution at  $\rho < 0.5$  and neoclassical contribution reduces down to ~20% at  $\rho = 0.8$ .

Figure 8 shows comparisons of experimental and neoclassical thermal conductivities. As shown in Fig. 8 (a),  $\chi_{e \text{ exp}}$  is lower in W7-X due to the steeper  $T_e$  gradient at comparable density.  $\chi_{e \text{ exp}}$  becomes comparable at  $\rho \sim 0.6$ . As shown in Fig. 6 (b),  $\chi_i$  is lower in W7-X at most of the location. Both in electron and ion channel, neoclassical contribution is much higher in LHD than in W7-X. This makes difficult to argue the difference of anomalous transport from  $\chi_{e \text{ exp}}$  and  $\chi_{i \text{ exp}}$ . Thus, the contributions of anomalous transport are investigated from  $\chi_{e \text{ exp}} - \chi_{e \text{ ano}}$  and  $\chi_{i \text{ exp}} - \chi_{i \text{ ano}}$ . There is an argument of this definition. For example,  $\chi_{i \text{ neo}}$  exceeds  $\chi_{i \text{ exp}}$  at  $\rho < 0.5$  in LHD as shown in Fig.8 (b), then  $\chi_{i \text{ exp}} - \chi_{i \text{ ano}}$  becomes negative. Also, at the location, where transport is dominated by neoclassical transport, still turbulence is clearly measured. Thus, neoclassical and turbulence transport may not be possible to add or subtract simply. However, for the present investigation of turbulence driven transport,  $\chi_{e \text{ exp}} - \chi_{e \text{ ano}}$  and  $\chi_{i \text{ exp}} - \chi_{i \text{ ano}}$  are used as a proxy of anomalous contribution. Figure 9 shows comparisons of possible contribution of anomalous transport. As shown in Fig. 9, at most of the locations, anomalous contributions are lower in LHD. In W-7X, negligible ETG contribution is realized only for  $a/L_{Te} \sim a/L_{Ti}$ . However, at  $\rho < 0.6$ ,  $a/L_{Te}$  is higher than  $a/L_{Ti}$ , thus, ETG can contribute the electron transport as well as ITG/TEM. In LHD, linear analyses shows both ITG and ETG are unstable. The 2D-PCI and microwave high k backscattering shows ion and electron scale turbulence [26]. Thus, both ITG/TEM and ETG can contribute the electron transport at  $\rho < 0.8$ , where  $a/L_{Te} > a/L_{Ti}$ . Therefore correspondence between simulation and electron transport is difficult to argue, because both ITG and ETG can contribute. On the other hand, ion transport can be governed by ITG or TEM. In W7-X, the dominant instability is not clarified yet, but ITG is likely dominant instability because density gradient is not steep. In LHD, dominant instability is ITG at  $\rho = 0.5$  and 0.7. Thus, the ITG simulation results shown in Fig.3 quantitatively agree with experimental observations.

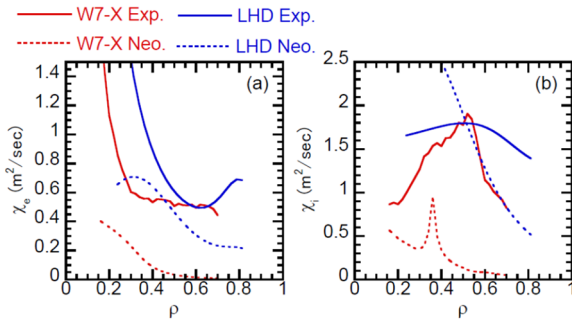


FIG.8 Comparisons of (a) electron thermal conductivities ( $\chi_e$ ) and (b) ion thermal conductivities ( $\chi_i$ ). Plain lines indicate experimental values, dashed line indicate neoclassical values.

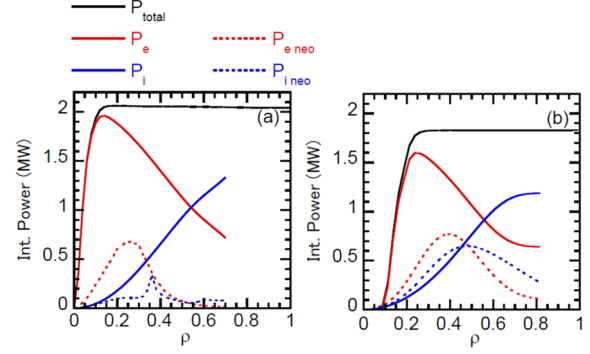


FIG.7 Integrated deposition power (a) W7-X and (b) LHD. Black plain lines indicate total deposition power, red and blue plain lines indicate electron and ion deposition power, red and blue dashed lines indicate neoclassical contribution.

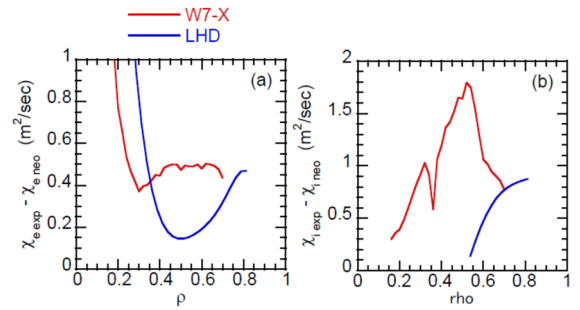


FIG.9 Possible contribution of anomalous transport (a) electron channel and (b) ion channel

## 4. SUMMARY

The configuration effects on transports were investigated in LHD and W7-X. Gyrokinetic non linear simulation shows lower ETG driven transport in W7-X than in LHD and lower ITG driven transport in LHD than in W7-X. Lower ETG driven transport in W7-X are due to the break of radial streamer. The lower ITG driven transport in LHD is due to the stronger generation of zonal flow. Configuration scan with different magnetic axis position in LHD shows simultaneous reduction of experimental  $\chi_e$  and neoclassical  $\chi_e$  associated with reduction of ion scale turbulence. The identical experiments in W7-X and LHD were performed. The density profiles are clearly different. It is peaked in W7-X and hollowed in LHD. This is likely due to the difference of amount of neoclassical thermo-diffusion. The electron temperature is more steepen in W7-X and  $T_i$  is similar at  $\rho < 0.6$ . The experimental  $\chi_e$  and  $\chi_i$  were lower in W7-X at most of the location, however, excluding neoclassical contribution, turbulence driven transport are lower both in electron and ion channel at most of radial locations. Lower anomalous contributions of ion transport in LHD is possibly due to the larger zonal flow generation indicated by gyrokinetic non-linear simulations. Among LHD configuration, lower  $\varepsilon_{\text{eff}}$  results in reduced transport, however, this dependence cannot be applicable for W7-X, because anomalous contribution in W7-X, with low  $\varepsilon_{\text{eff}}$  is higher than in LHD. The configuration optimization to reduce turbulence driven anomalous transport require further investigations to find ruling parameter of magnetic properties.

## REFERENCES

- [1] MIYAMOTO, K., Plasma Physics for Controlled Fusion, Springer Series on Atomic, Optical, and Plasma Physics book series (2016)
- [2] MURAKAMI, S., et al, “Neoclassical transport optimization of LHD”, Nucl. Fusion **42** (2002) L19–L22
- [3] BEIDLER, C. D., et al, “Benchmarking of the mono-energetic transport coefficients—results from the International Collaboration on Neoclassical Transport in Stellarators”, Nucl. Fusion **51** (2011) 076001
- [4] SUGAMA, H., WATANABE, T. H., “Dynamics of Zonal Flows in Helical Systems”, Phys. Rev. Lett., **94**, (2005) 115001
- [5] WATANABE, T. H., H. SUGAMA, H., FERRANDO-MATGALET, S., “Reduction of Turbulent Transport with Zonal Flows Enhanced in Helical Systems”, Phys. Rev. Lett., **100**, (2008) 195002
- [6] YAMADA, H., “Characterization of energy confinement in net-current free plasmas using the extended International Stellarator Database”, Nucl. Fusion **45** (2005) 1684–
- [7] PROLL, J. H. E., HELANDER, P., CONNOR, J. W., et al. “Resilience of Quasi-Isodynamic Stellarators against Trapped-Particle Instabilities”, Physical Review Letters, **108**, (2012) 245002
- [8] XANTHOPOULOS, P., BOZHENKOV, S. A., BEURSKENS, M. N., et al. “Turbulence Mechanisms of Enhanced Performance Stellarator Plasmas”, Phys. Rev. Lett., **125**, (2020) 075001
- [9] KURODA, T., SUGAMA, H., et al, “Ion Temperature Gradient Modes in Toroidal Helical Systems”, Journal of the Physical Society of Japan, **69** (2000) 2485
- [10] PLUNK, G. G., XANTHOPOULOS, P., WEIR, G. M., et al. “Stellarators Resist Turbulent Transport on the Electron Larmor Scale”, Phys. Rev. Lett., **122**, (2019) 035002
- [11] WERMER, F., TANAKA, K., XANTHOPOULOS, P., NUNAMI, M., et al, “Impact of Magnetic Field Configurations on Heat Transport in Stellarators”, to be submitted
- [12] NUNAMI, M., WATANABE, T. H., SUGAMA, H., “Gyrokinetic Vlasov Code Including Full Three-dimensional Geometry of Experiments”, Plasma and Fusion Research, **5**, (2010) 016
- [13] JENKO, F., DORLAND, W., KOTSCHENREUTHER, M., et al. “Electron temperature gradient driven turbulence”, Physics of Plasmas, **7**, (2000), 1904
- [14] JENKO, F., KENDLE, A., “Radial and zonal modes in hyperfine-scale stellarator turbulence”, Physics of Plasmas, **9**, (2002) 4103
- [15] WEIR, G. M., XANTHOPOULOS, P., et al, “Heat pulse propagation and anomalous electron heat transport measurements on the optimized stellarator W7-X”, Nucl. Fusion **61** (2021) 056001
- [16] YAMADA, I., NARIHARA, K., FUNABA, H., et al. “Recent Progress of the LHD Thomson Scattering System”, Fusion Science and Technology, **58**, (2010) 345
- [17] YOSHINUMA, M., IDA, K., YOKOYAMA, M., et al. “Charge-Exchange Spectroscopy with Pitch-Controlled Double-Slit Fiber Bundle on LHD”, Fusion Science and Technology, **58**, (2010), 375
- [18] TANAKA, K., KAWAHATA, K., TOKUZAWA, T., et al. “Particle Transport of LHD”, Fusion Science and Technology, **58**, (2010), 70

- [19] OHTANI, Y., TANAKA, K., et al. "Particle transport of electron cyclotron resonant heating plasma in Large Helical Device", *Plasma Physics and Controlled Fusion*, **62**, (2020), 025029
- [20] SEKI, R., et al, "Transport Study of LHD High-Beta Plasmas Based on Power Balance Analysis with TASK3D Code Module", *Plasma Fusion Res.* 6 (2011) 2402081
- [21] TANAKA, K., MICHAEL, C. A., VYACHESLAVOV, L. N., et al, "Two-dimensional phase contrast imaging for local turbulence measurements in large helical device", *Review of Scientific Instruments*, **79**, (2008) 10E702
- [22] MICHAEL, C. A., TANAKA, K., VYACHESLAVOV, L. N., et al, "Two-dimensional wave-number spectral analysis techniques for phase contrast imaging turbulence imaging data on large helical device", *Review of Scientific Instruments*, **86**, (2015), 093503
- [23] TANAKA, K., KAWAHATA, K., TOKUZAWA, T., et al. "Density Reconstruction Using a Multi-Channel Far-Infrared Laser Interferometer and Particle Transport Study of a Pellet-Injected Plasma on the LHD", *Plasma and Fusion Research*, **3**, (2008), 050
- [24] PASCH, E., BEURSKENS M. N. A., BOZHENKOV, S. A., et al. "The Thomson scattering system at Wendelstein 7-X", *Review of Scientific Instruments*, vol. 87, no. 11, p. 11E729 (2016)
- [25] FORD, O. P., L. VANO, J., ALONSO, A., et al. "Charge exchange recombination spectroscopy at Wendelstein 7-X", *Review of Scientific Instruments*, **91**, (2020) 023507
- [26] TANAKA, K., NAKATA, M., et al. "Extended investigations of isotope effects on ECRH plasma in LHD", *Plasma Physics and Controlled Fusion*, **62**, (2020), 024008
- [27] TOKUZAWA, T., to be published *Review of Scientific Instruments*
- [28] ALCUSON, J. A., XANTHOPOULOS, P., PLUNK, G. G., et al. "Suppression of electrostatic micro-instabilities in maximum-J stellarators", *Plasma Physics and Controlled Fusion* **62**, (2020) 035005.